Journal of Alloys and Compounds 488 (2009) 144–147

Contents lists available at ScienceDirect

Journal of Alloys and Compounds

journal homepage: www.elsevier.com/locate/jallcom

Mechanochemical synthesis of $(Fe,Ti)_3Al$–Al_2O_3 nanocomposite

M. Rafiei, M.H. Enayati*, F. Karimzadeh

Department of Materials Engineering, Isfahan University of Technology, Isfahan 84156-83111, Iran

ARTICLE INFO

Article history:
Received 30 July 2009
Received in revised form 1 September 2009
Accepted 2 September 2009
Available online 8 September 2009

Keywords:
Composite materials
Intermetallics
Nanostructured materials
Mechanical alloying

ABSTRACT

Formation mechanism of $(Fe,Ti)_3Al$–Al_2O_3 nanocomposite prepared by mechanical alloying of Fe, Al and TiO_2 with molar ratio of 6:7:3 was studied. The structural changes of powder particles during mechanical alloying were investigated by X-ray diffractometery. Morphology and microstructure of powder particles were characterized by scanning electron microscopy. It was found that during mechanical alloying Al first reacts with TiO_2 leading to the gradual formation of crystalline Ti and amorphous Al_2O_3 phases. In the second stage Ti and remaining Al diffuse into the Fe lattice and as a result a Fe(Al,Ti) solid solution develops. This structure transformed to $(Fe,Ti)_3Al$ intermetallic compound at longer milling times. Heat treatment of this structure led to the crystallization of Al_2O_3 and ordering of $(Fe,Ti)_3Al$ phases.

1. Introduction

Fe_3Al based intermetallics indicate attractive properties including, high hardness, high melting point, relatively low density compared with Fe- and Ni-based alloys and excellent oxidation and corrosion resistance [1]. As a result these compounds are useful for many structural applications including, gas metal filters, heating element, heat treatment fixtures, high temperature dies and molds and cutting tools [2,3]. Addition of third alloying element such as Ti, Cr, ... to Fe_3Al intermetallic compound can lead to the improvement of mechanical properties including ductility at room temperature and creep resistance at high temperature, chemical stability and tribological behavior by solid solution and/or precipitation hardening as well as grain boundary strengthening [4–6].

Moreover it was shown that the dispersion of a hard second phase material (e.g., Al_2O_3) within the matrix can enhance the mechanical properties [7]. Intermetallic reinforced alumina composites exhibit several advantages such as; high strength, good wear resistance and improved fracture toughness [8,9].

There have been several investigations on preparation of titanium aluminides and iron aluminides matrix nanocomposites by mechanical alloying (MA) but, no study on synthesis of $(Fe,Ti)_3Al$ matrix nanocomposite was reported in the literature. Zhang et al. [10] reported that MA of Al–TiO_2 powder mixture leads to the formation of a rang of Ti-based composites including $Ti(Al,O)/Al_2O_3$, $Ti_xAl_y(O)/Al_2O_3$ and Ti_3Al/TiAl.

Forouzanmehr et al. [11] synthesized the $TiAl/Al_2O_3$ nanocomposite by MA of Al and TiO_2 powder mixture and reported that TiO_2 is gradually reduced by Al during ball milling. Khodaei et al. [12] synthesized Fe_3Al–Al_2O_3 nanocomposite by MA of Al and Fe_2O_3 powder mixture and reported that prior to the Fe_2O_3–Al combustion reaction, powder particles attained a nanocrystalline structure which promotes the Fe_2O_3–Al reaction by providing high diffusivity paths.

In our previous work [13] the formation of $(Fe,Ti)_3Al$ intermetallic compound was discussed. In this work the formation mechanism of $(Fe,Ti)_3Al$–Al_2O_3 nanocomposite by MA starting from Fe, Al and TiO_2 powder mixture is reported.

2. Experimental

Fe, Al and TiO_2 powder mixture with purity of 99.8%, 99.5% and 99%, respectively were used as starting materials. The Fe powder particles had a nearly uniform size of ~100 μm. Al particles were irregular in shape with a size distribution of 50–100 μm and TiO_2 particles were very fine with a size distribution of 200–300 nm.

The Fe, Al and TiO_2 powders with molar ratio of 6:7:3 were mixed according to the reaction (1). MA was carried out in a high energy planetary ball mill, nominally at room temperature and under Ar atmosphere. The milling media consisted of five 20 mm diameter balls confined in a 120 ml volume vial. The ball and vial materials were hardened chromium steel. Ball to powder weight ratio and rotation speed of vial were 10:1 and 500 rpm, respectively. The total powder mass was 18 g with 0.3 wt.% stearic acid as a process control agent (PCA). Samples were taken at selected time intervals and characterized by X-ray diffraction (XRD) in a Philips X' PERT MPD diffractometer using filtered Cu K_α radiation ($\lambda = 0.1542$ nm). Morphology and microstructure of powder particles were characterized by scanning electron microscopy (SEM) in a Philips XL30. The mean powder particle size was estimated from SEM images of powder particles by image tool software. The average size of about 30 particles was calculated and reported as mean powder particle size.

Isothermal annealing was carried out to study the thermal behavior of milled powders. A small amount of powder was sealed and isothermally annealed at 900 °C for 1 h in a conventional furnace and then cooled in air. The structural transition

* Corresponding author. Tel.: +98 311 3915730; fax: +98 311 3912752.
E-mail address: ena78@cc.iut.ac.ir (M.H. Enayati).

0925-8388/$ – see front matter © 2009 Elsevier B.V. All rights reserved.
doi:10.1016/j.jallcom.2009.09.007

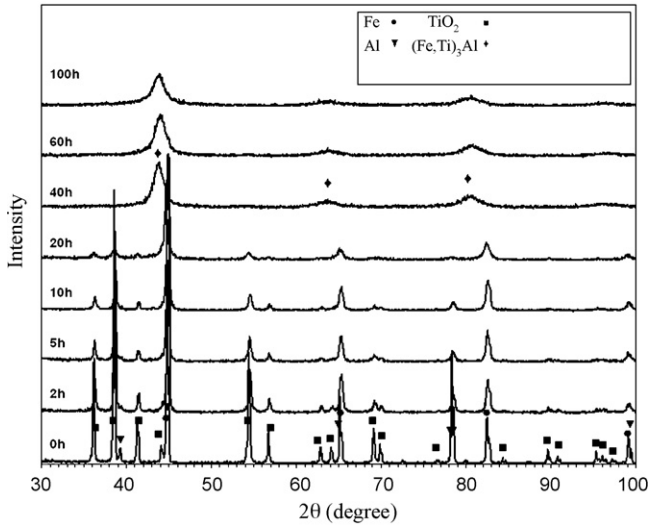

Fig. 1. XRD patterns of Fe, Al and TiO_2 powder mixture at different milling times.

occurred during annealing were determined by XRD. The crystallite size and internal strain of powders were estimated using the Williamson–Hall method [14].

3. Results and discussion

3.1. Structural evolution

$(Fe,Ti)_3Al$–35 vol.% Al_2O_3 nanocomposite can be synthesized starting from Fe, Al and TiO_2 powder mixture according to the following reaction:

$$6Fe + 7Al + 3TiO_2 = 3(Fe, Ti)_3Al + 2Al_2O_3 \quad (1)$$

Fig. 1 shows XRD patterns of Fe, Al and TiO_2 powder mixture as-received and after different milling times. XRD results suggest that the reaction (1) takes place in two subsequent stages;

$$4Al + 3TiO_2 = 3[Ti]_{Fe} + 2Al_2O_3 \quad (2)$$

$$6Fe + 3[Al]_{Fe} + 3[Ti]_{Fe} = 3(Fe, Ti)_3Al \quad (3)$$

As can be seen with increasing milling time the intensity of Fe, Al and TiO_2 diffraction peaks decreases and their width increases due to the internal strain induced by lattice defects and refinement of crystallite size. Moreover Fe (1 1 0) diffraction peak gradually displaced toward lower angles. During milling Al can react with TiO_2 according to the reaction (2).

ΔG°_{298} for reaction (2) has a very high negative value (−498212 J/mol) indicating that reaction (2) can thermodynamically take place at room temperature. However reactions with negative ΔG°_{298} do not necessarily occur at room temperature because of their slow kinetic. In this regard MA can enhance kinetics of reactions by creating high diffusivity paths, providing extensive interface area between reactants and by the dynamic removing of reaction product at interfaces due to the repeated fracturing and cold welding of powder particles and local temperature rise [15].

The displacement of Fe (1 1 0) peak toward lower angles (Fig. 2) after 20 h of MA suggests that Ti formed by reaction (2) and remaining Al dissolve into Fe lattice according to the reaction (3) and therefore a Fe(Al,Ti) solid solution forms during milling. Increasing milling time to 40 h led to the transformation of Fe(Al,Ti) solid solution to $(Fe,Ti)_3Al$ intermetallic compound which is accompanied by a change in XRD peaks position (Fig. 1). Similar behavior was observed during MA of Fe, Al and Ti ternary system [13]. It should be noted that the Al_2O_3 XRD peaks formed by reaction (1) cannot be observed on XRD patterns (Fig. 1). In fact in-situ formed Al_2O_3 particles are expected to have a very small size with an amorphous structure [16,17]. Formation of amorphous Al_2O_3 phase during ball milling of Al and TiO_2 powder mixture was previously reported [11].

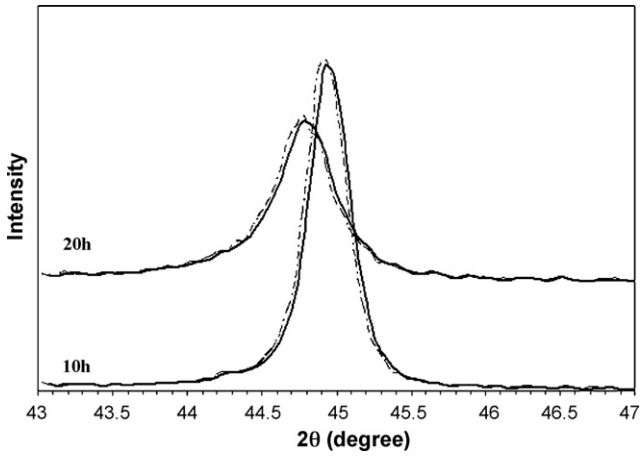

Fig. 2. Displacement of Fe(1 1 0) diffraction peak.

Table 1
Crystallite size and internal strain of $(Fe,Ti)_3Al$ phase at different milling times.

Milling time (h)	Crystallite size (nm)	Internal strain (%)
40	20	2
60	12	2
100	10	2

Lack of superlattice diffraction peaks for $(Fe,Ti)_3Al$ phase indicates that this phase has a disordered crystal structure. Increasing milling time up to 100 h has no significant effect on phase composition, but increased the broadening of XRD peaks. Crystallite size and internal strain of $(Fe,Ti)_3Al$ phase at different milling times are given in Table 1. As seen the $(Fe,Ti)_3Al$ crystallite size decreases with increasing milling time.

3.2. Thermodynamics aspects

As mentioned reaction (1) takes place in two subsequent stages. First stage, reaction (2), has negative ΔG°_{298} and ΔH°_{298} values indicating that this reaction can occur at room temperature and is highly exothermic. The adiabatic temperature (T_{ad}) is often used

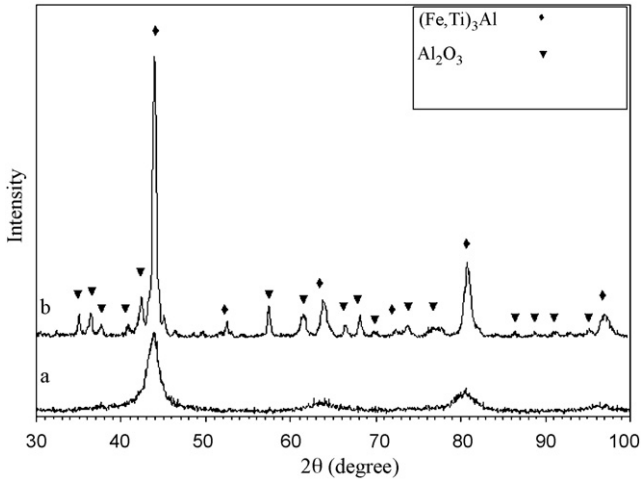

Fig. 3. XRD patterns of Fe, Al and TiO_2 powder mixture (a) after 100 h milling and (b) after heat treatment at 900 °C for 1 h.

as a criterion for anticipation of modality of reactions [18]. T_{ad} is the highest temperature that the reaction system can reach, provided that all the released heat is used to increase the temperature of system after the initiation of reaction [19]. It has been empirically demonstrated that the reaction will be self-sustaining only if $T_{ad} \geq 1527\,^{\circ}C$ [20].

The value of T_{ad} for reaction (2) was calculated to be about 1532 °C [19]. Therefore reaction (2) is expected to occur with a combustion mode during ball milling. The addition of diluents will however decrease the T_{ad} [19]. In this work extra Fe and Al were added to the starting powder mixture to obtain $(Fe,Ti)_3Al$ matrix. In this case T_{ad} was calculated using following relation:

$$-\Delta H^{\circ}_{298} = 2\int_{298}^{T_{ad}} C_p^{Al_2O_3}\,dT + 3\int_{298}^{T_{ad}} C_p^{Ti(\alpha)}dT + 6\int_{298}^{T_{ad}} C_p^{Fe(\alpha)}\,dT + 3\int_{298}^{933} C_p^{Al(s)}dT + 3\times\Delta H_{Al}{}^{m} + 3\int_{933}^{T_{ad}} C_p^{Al(l)}dT \quad (4)$$

where in this equation ΔH°_{298} is the enthalpy change of reaction at room temperature, C_p the heat capacity and $\Delta H_{Al}{}^{m}$ the enthalpy of fusion of Al. The T_{ad} in presence of extra Fe and Al was calculated to be 787 °C indicating that the modality of reaction (2) is gradual (progressive) rather than self-propagating combustion.

As seen in Fig. 3 after isothermal annealing (900 °C, 1 h) of 100 h milled sample the Al_2O_3 peaks are observed on XRD pattern. The appearance of crystalline Al_2O_3 peaks can further confirm that the Al_2O_3 formed during ball milling has an amorphous structure which subsequently transforms to a crystalline structure during annealing. Also the presence of $(Fe,Ti)_3Al$ superlattice diffraction peaks in annealed sample implies that the degree of DO_3 ordering increases during annealing.

The crystallite size and internal strain of $(Fe,Ti)_3Al$ and Al_2O_3 phases after heat treatment are given in Table 2.

Table 2
Crystallite size and internal strain of $(Fe,Ti)_3Al$ and Al_2O_3 phases after heat treatment at 900 °C for 1 h.

Phase	Crystallite size (nm)	Internal strain (%)
$(Fe,Ti)_3Al$	70	0.85
Al_2O_3	55	0.75

3.3. Morphological changes

Morphological changes of powder particles during milling were analyzed by SEM observations. As can be seen in Fig. 4 after 2 and 5 h of milling times the powder particles were irregular in shape with non-uniform size distribution. The mean powder particle size after 2 h of milling time was about 45 μm which reduced to 35 μm as milling time increased to 5 h. On further milling the powder particle size continuously decreased and became more uniform so that after 100 h of milling time the mean powder particle size was about 10 μm. The very fine powder particles (Fig. 4c and e) formed at final stage of milling are as a result of formation of $(Fe,Ti)_3Al$ and Al_2O_3 brittle phases as confirmed by XRD results (Fig. 1). It should be noted that the larger particles in this stage are an agglomeration of many smaller particles.

3.4. Microstructural studies

Fig. 5 shows cross-sectional SEM images of powder particles after different milling times. As can be seen after 2 h of milling time a composite microstructure consisting of cold welded Fe, Al and TiO_2 phases is formed. At early stage this structure is coarse and non-uniform. Increasing milling time to 5 h led to the refinement of composite microstructure as a result of repeated cold welding and fracturing of powder particles. This fine microstructure includes an extensive interface area between Fe, Al and TiO_2 phases which promotes the interdiffusion of atoms through high diffusivity paths

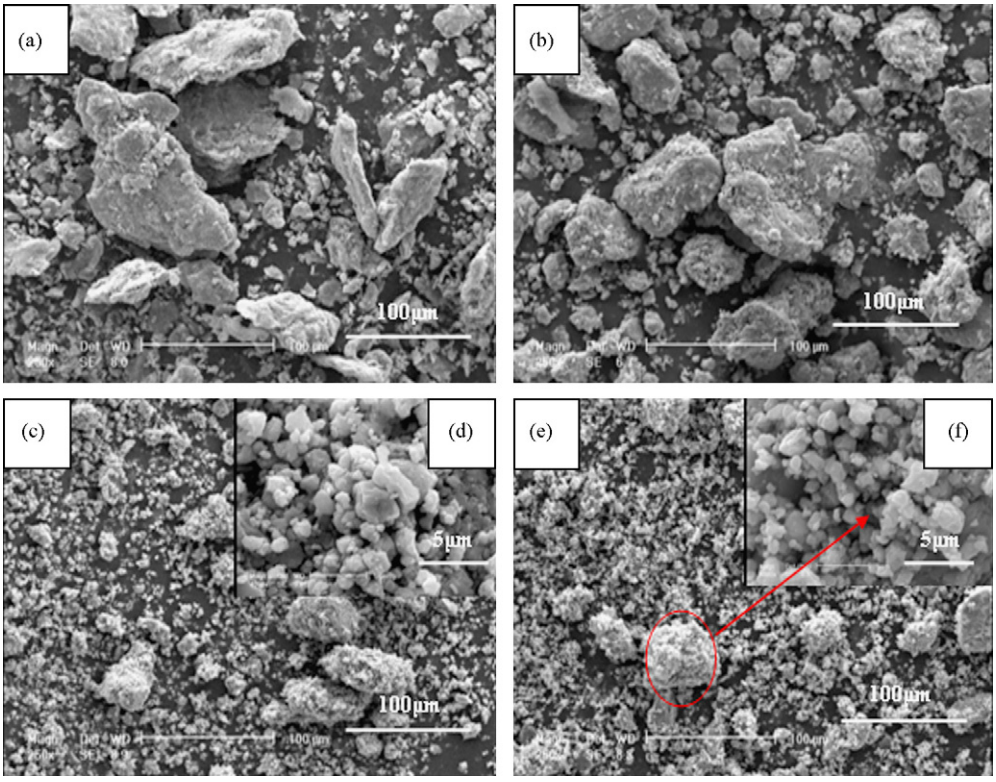

Fig. 4. SEM images of powder particles after (a) 2 h, (b) 5 h, (c and d) 60 h and (e and f) 100 h of milling times.

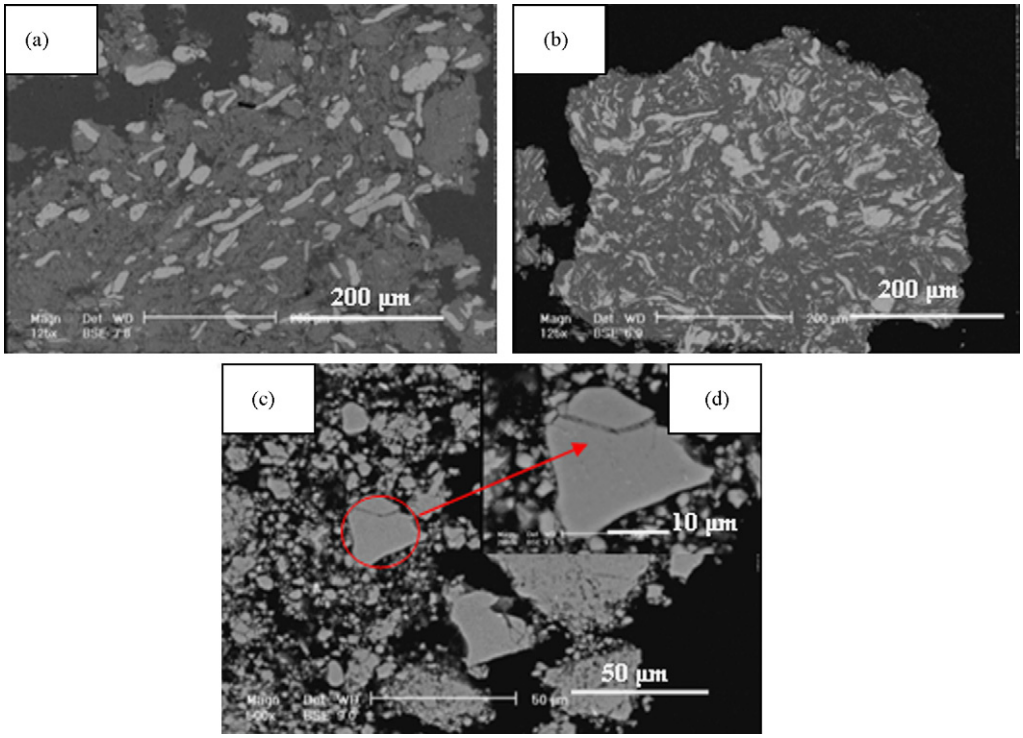

Fig. 5. Cross-sectional SEM images of Fe, Al and TiO_2 powder mixture after (a) 2 h, (b) 5 h (c and d) 60 h of milling times.

(dislocations and grain boundaries) and therefore can increase the reaction kinetics at ambient temperature. At longer milling times a featureless microstructure is observed on SEM (Fig. 5c and d) indicating that $(Fe,Ti)_3Al–Al_2O_3$ nanocomposite is completely formed in consistence with XRD results.

4. Conclusion

Mechanical alloying of Fe, Al and TiO_2 powder mixture led to the formation of $(Fe,Ti)_3Al–Al_2O_3$ nanocomposite. It was found that the TiO_2 oxide is gradually reduced by Al during milling. This reaction led to the formation of crystalline Ti and amorphous Al_2O_3. On further milling Ti (reduced from TiO_2) and remaining Al dissolved into Fe lattice and formed a Fe(Al,Ti) solid solution which transformed to $(Fe,Ti)_3Al$ intermetallic compound with disordered DO_3 structure at longer milling times. Annealing of final structure led to the crystallization of amorphous Al_2O_3 and ordering of $(Fe,Ti)_3Al$ matrix.

References

[1] K. Matsuura, Y. Obara, M. Kudoh, ISIJ. Int. 46 (2006) 871–874.
[2] J.R. Knibloe, R.N. Wright, V.K. Sikka, R.H. Baldwin, C.R. Howell, Mater. Sci. Eng. A 153 (1992) 382–386.
[3] K. Yoshimi, S. Hanada, JOM (1997) 46–49.
[4] S.M. Zhu, M. Tamura, K. Sakamoto, K. Iwasaki, Mater. Sci. Eng. A 292 (2000) 83–89.
[5] R.T. Fortnum, D.E. Mikkola, Mater. Sci. Eng. A 9 (1987) 223–231.
[6] M.G. Mendiratta, S.K. Ehlers, H.A. Lipsitt, Metall. Trans. A18 (1987) 509–518.
[7] N.J. Welham, Intermetallics 6 (1998) 363–368.
[8] S. Schicker, D.E. Garcia, I. Gorlov, R. Janssen, N. Claussen, J. Am. Ceram. Soc. 82 (1999) 2607–2612.
[9] D. Horvitz, I. Gotman, E.Y. Gutmanas, N. Claussen, J. Eur. Ceram. Soc. 22 (2002) 947–954.
[10] D.L. Zhang, Z.H. Cai, G. Adam, JOM (2004) 53–56.
[11] N. Forouzanmehr, F. Karimzadeh, M.H. Enayati, J. Alloys Compd. 478 (2009) 257–259.
[12] M. Khodaei, M.H. Enayati, F. Karimzadeh, J. Alloys Compd. 467 (2009) 159–162.
[13] M. Rafiei, M.H. Enayati, F. Karimzadeh, J. Alloys Compd. 480 (2009) 392–396.
[14] G.K. Williamson, W.H. Hall, Acta. Metall. 1 (1953) 22–31.
[15] C. Suryanarayana, Prog. Mater. Sci. 46 (2001) 1–184.
[16] J.M. Wu, Mater. Lett. 48 (2001) 324–330.
[17] M. Uma Devi, Ceram. Int. 30 (2004) 555–565.
[18] N.Q. Wu, Mater. Sci. Technol. 14 (1997) 287–292.
[19] Y. Li, Z. Zheng, J. Mater. Sci. Technol. 15 (1999) 271–275.
[20] Z. Peng-lin, X. Tian-dong, Z. Guo-dong, Y. Li-jing, Z. Wen-jun, Trans. Nonferr. Met. Soc. China 17 (2007) 27–31.